Journal of Solid State Chemistry **149,** 113–119 (2000)
Article ID jssc.1999.8504, available online at http://www.idealibrary.com on IDEAL®

Effect of Addition of Divalent Transition Metal Chlorides on the Structure and Thermal Stability of Lamellar Silica Synthesized by the Neutral Amine Route

Robson F. de Farias*,[1] and Claudio Airoldi†,[2]

*Departamento de Química, Universidade Federal de Roraima, 69310–270 Boa Vista, Roraima, Brasil; and †Instituto de Química, Universidade Estadual de Campinas, Caixa Postal 6154, 13083–970 Campinas, São Paulo, Brasil

Received May 18, 1999; in revised form September 8, 1999; accepted September 15, 1999

The addition of divalent metal chlorides MCl_2 (M = Mn, Co, Ni, Cu, Zn, Cd, Hg) drastically affects the structure and thermal stability of lamellar silica obtained through the neutral amine route using 1,12-diaminedodecane as template molecule. These changes in properties are related to the coordination features, as well as the amount of cation employed. The enhancement of the thermal stability of the modified lamellar silica is always independent of the cation added. On the other hand, the thermal stability of the hexagonal phase decreased. The occurrence of structural changes can be attributed to the reorientation of 1,12-diaminedodecane chains to allow cation coordination through nitrogen atoms. © 2000 Academic Press

INTRODUCTION

Because it can be used to synthesize, at room temperature, a series of new materials with homogeneous and variable composition, the sol–gel process (1) is increasingly being used as a synthetic route in materials chemistry research (2–11). In this connection, the sol–gel method can be successfully employed to prepare lamellar inorganic–organic hybrid compounds from alkyltrimethylammonium bromide salts (12–15) or neutral *n*-alkyldiamines (16, 17) as template molecules, by including some silicon or transition metal alkoxides. However, in the synthetic route for neutral *n*-alkyldiamines, template chain length and solvent composition, mainly water content, play a crucial role in formation of the final product, which could be derived to lamellar or hexagonal silicas (16).

Since free nitrogen atoms in *n*-alkyldiamine chains have strong ability in coordinating metal cations, investigations on the effect of addition of metal salts on the structure and thermal stability of the lamellar silica formed can provide important information about the physical behavior of this kind of material.

We report the synthesis of and corresponding modification with transition metal chlorides, MCl_2 (M = Mn, Co, Ni, Cu, Zn, Cd, Hg), of lamellar silica using the so-called neutral amine route through the sol–gel process. The aim of this investigation is to provide some experimental insight into the effects exerted by metal addition on the structure and thermal stability of the synthesized hybrids. Another purpose is to establish a series of experimental procedures that allow the synthesis of materials with a desired structure and thermal stability of the final product.

EXPERIMENTAL

All reagents used were of analytical grade and were employed without further purification.

The lamellar silica was prepared by the following procedure: 1.0×10^{-2} mol of 1,12-diaminedodecane was added to 0.50 mol of *n*-propanol. To this homogeneous solution 3.30 mol of water was slowly added. This final mixture was stirred about 10 mins to obtain a homogeneous phase, to which 1.0×10^{-2} mol of tetraethylorthosilicate was added. The resulting product was aged for 24 h at room temperature, then filtered and dried under vacuum at 80°C for 5 h. This final lamellar matrix is designated here as LS.

LS was chemically modified by introducing cations by the following experimental procedure. The general preparation consisted of adding a desired amount of a given metal chloride to the final aged gel. This suspension was magnetically stirred for 2 h, and the solid was filtered and dried under vacuum at 80°C for 5 h. Samples of the supernatant solution were titrated in duplicate using a standard 0.020 mol dm^3 EDTA solution (18), to determine the total amount of cation bonded to the matrices. Two distinct modified silica samples containing copper chloride were synthesized to adjust to 10.0 and 15.0 mmol of this salt bonded to the matrices. Only one sample each of the divalent Mn, Co, Ni,

[1] Present address: Instituto de Química, Universidade Estadual de Campinas, Caixa Postal 6154, 13083–970 Campinas, São Paulo, Brasil.

[2] To whom correspondence should be addressed.

0022-4596/00 $35.00

Zn, Cd, Hg chlorides (10.0 mmol) was obtained, and the matrices are designated as LSCu1, LSCu2, LSMn, LSCo, LSNi, LSZn, LSCd, and LSHg, respectively.

X-Ray diffraction patterns were recorded with a Shimadzu apparatus using Cu$K\alpha$ radiation. Thermogravimetric and DSC data were obtained with Shimadzu TGA50 and DuPont apparatus, respectively. Both analyses were performed under an argon atmosphere and at a heating rate of 8.3×10^{-2}°C s^{-1}. Scanning electron microscopy images were obtained using Jeol equipment (Model JSM T-300) at an accelerating voltage of 20 kV. Infrared spectra were obtained with Bomem equipment in the range 4000–400 cm^{-1} as KBr pellets. ^{29}Si NMR cross-polarization (CP)/magic-angle spinning (MAS) spectra of solid samples were obtained using a Bruker AC 300/P instrument at room temperature, under the following experimental conditions: pulse repetition time = 0.115 s, contact time = 3 ms, accumulations = 17,857.

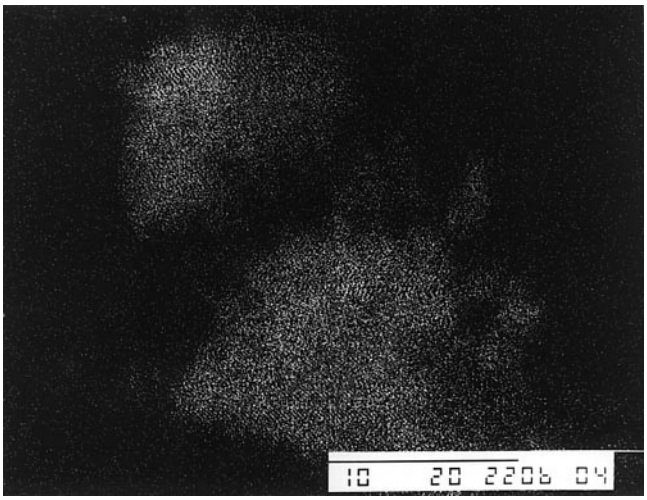

FIG. 1. SEM mapping image of the distribution of copper atoms on the surface of the LSCu2 hybrid. Scale Bar is in micrometers.

RESULTS AND DISCUSSION

The combination of magic-angle spinning (MAS) and cross-polarization (CP) provides ^{29}Si NMR spectra with a high degree of structural resolution, permitting the acquisition of details on the structure and transformation of the silica surface (19, 20). For a normal silica gel sample the sequence of peaks at −89, −100, and −109 ppm can be assigned to geminal silanols, $(>SiO)_2Si(OH)_2$, single silanols, $(>SiO)_3SiOH$, and surface silicon groups, $(>SiO)_4Si$, respectively (19, 20). For the synthesized lamellar silica, as well as for all the metal-doped samples, these three peaks are located near the same positions, with deviation of ±2 ppm, which is an acceptable range of experimental error. Based on these experimental results, it can be concluded that the silica substrate in undoped and doped matrices is composed of amorphous silica. The crystallinity of the inorganic–organic hybrids is a consequence of the presence of the template molecules, which organize the structure of the compounds.

The mapping corresponding to SEM images for all the doped hybrids showed that the metal is homogeneously distributed on the grains of the hybrid matrices. An illustration for the LSCu2 sample is shown in Fig. 1. The profile of this image is in agreement with a lamellar structure for the copper-doped hybrid.

The main infrared bands for 1,12-diaminedodecane, as well as for all the hybrid matrices synthesized, are listed in Table 1. The bands associated with the amino groups are those assigned to 3170 and 3256 cm^{-1}, which are characteristic of NH stretching of primary amines (21), as well as the band at 1609 cm^{-1} corresponding to the characteristic scissoring vibration mode. As observed in Table 1 the CH_2 group vibration modes remain pratically unchanged in the lamellar silica in all metal-doped hybrids. On the other hand, significant shifts can be observed for the bands associated with the amino groups. With the exception of the LSHg matrix, for which the frequency of the asymmetric νNH vibration decreases, all the hybrids presented the same vibration mode with a shift to higher frequency values. However, for the symmetric vibration mode, normal behavior could not be observed.

X-Ray diffraction patterns of the original lamellar silica and of lamellar silica doped with 10.0 and 15.0 mmol of $CuCl_2$ are shown in Fig. 2. The X-ray diffraction data for all matrices obtained are summarized in Table 2. For the lamellar silica in Fig. 2a three diffraction peaks are observed at 2θ values of 3.8°, 7.3°, and 11.5° attributed to the 001, 002, and 003 diffraction planes (16, 17), which correspond to d spacings of 2.3, 1.2, and 0.70 nm, respectively. However, an important feature to be considered is related to the disposition of the n-alkyldiamine molecule in the gallery space.

TABLE 1
Main Infrared Bands (cm^{-1}) for 1,12-Diaminedodecane (DAD), the Lamellar Silica (LS), and the Metal-Doped Silica Samples

Sample	νNH[a]	νCH_2(asym)	νCH_2(sym)	δNH	δCH_2
DAD	3256, 3170	2919	2849	1609	1462
LS	3361, 3297	2923	2852	1603	1468
LSMn	3403, 3206	2919	2850	1615	1469
LSCo	3401, 3020	2920	2848	1619	1467
LSNi	3441, 3036	2918	2851	1629	1471
LSCu1	3361, 3245	2912	2846	1584	1468
LSCu2	3357, 3136	2919	2850	1577	1461
LSZn	3451, 3141	2921	2851	1584	1483
LSCd	3276, 3258	2912	2850	1610	1417
LSHg	3192, 3108	2912	2848	1605	1470

[a] Asymmetric and symmetric vibration modes.

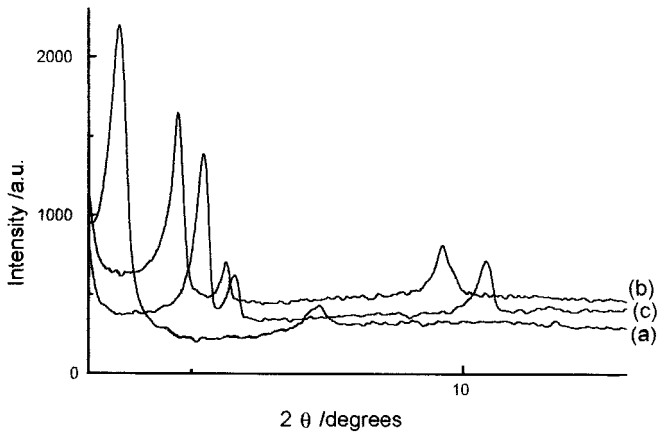

FIG. 2. X-Ray diffraction paterns of lamellar silica (a) and lamellar silica doped with 10.0 (b) and 15.0 (c) mmol of $CuCl_2$.

Therefore, the chain length of 1.15 nm for the amine mentioned can be calculated using covalent radius values for carbon, nitrogen, and hydrogen atoms. Based on this value, it can be inferred that two *n*-alkyldiamines are located in pairs, bonding in opposite inorganic sheets, with one molecule above the other, to give a linear top-to-tail arrangement, with the experimental value of 2.3 nm for the interlamellar distance.

The hybrids containing copper cations are shown in Figs. 2b and 2c, and exhibit the diffraction peaks due to the 001 and 002 planes at 4.7° and 5.1° (001) and 9.6° and 10.4° (002) for 10.0 and 15.0 mmol of cation in the matrix, respectively. These results confirmed that the lamellar nature of the original matrix is retained by the modified hybrids.

The hybrid that incorporated 10.0 mmol of copper gave a solid with a blue powder. This matrix shifted the 001 plane to 4.7°, which corresponds to a *d* spacing of 1.9 nm. This value clearly demonstrates that addition of metal halide caused a reorganization of the *n*-alkyldiamine chains, promoted by copper nitrogen atom coordination, and, consequently, the order of the silica framework was changed to allow the maximum sites of coordination. For the 15.0-mmol-doped material, a yellowish powder, a lamellar silica product resulted. As observed for the similar preceding hybrid, an identical structure was obtained, but all diffraction peaks were shifted to higher 2θ values. Thus, the 001 diffraction peak is shifted to 5.1° to give a *d* spacing of 1.7 nm. This value indicates that the diamine chains underwent a larger interlamellar reorganization as a consequence of the larger amount of cations introduced into the system. This consumption of cations can be explained by the facility of the free basic nitrogen atoms disposed the lamellar gallery to coordinate the available cations. However, the distribution of *n*-alkyldiamine chains undergoes another rearrangement due to the cation coordination and decrease in interlamellar spacing. This contraction can be explained by assuming that in normal coordination each copper cation can be bonded to four free nitrogen atoms disposed on the pendant *n*-alkyldiamine of two adjacent immobilized molecules. By using a simple geometrical consideration, the mean distance between adjacent diamine chains can be calculated with Pythagoras' theorem to give 1.3 nm for the 10.0-mmol-doped copper matrix, as is schematically represented in Fig. 3. In this condition, the chains are forced to an established inclination of 34.3° from the vertical position. A third diffraction peak is observed at 5.75° and 5.80° for the hybrids containing 10.0 and 15.0 mmol of copper, respectively. This peak is absent in the original hybrid and could be tentatively attributed to the 220 plane, which is characteristic of a cubic phase (22).

For the copper-modified hybrids, which contained distinct amounts of coordinated metal, differences in the

TABLE 2
X-Ray Diffraction Data for Lamellar Silica and Transition Metal Chloride-Doped matrices

Matrix	2θ (deg)	*d*-spacings (nm)	Diffraction planes
LS	3.8; 7.3; 11.5	2.3; 1.2; 0.7	001; 002; 003
LSMn	5.8	1.5	001
LSCo	5.9	1.5	001
LSNi	3.8[a]; 5.6; 11.4	2.3; 1.6; 0.8	001[a]; 001; 002
LSCu1	4.7; 5.8; 9.6	1.9; 1.5; 0.9	001; 220?; 002
LCCu2	5.1; 5.8; 10.4	1.7; 1.5; 0.8	001; 220?; 002
LSZn	5.8; 6.7	1.5	001?
LSCd	4.9; 9.7; 14.6	1.8; 0.9; 0.6	001; 002; 003
LSHg	4.8; 9.6; 14.4	1.8; 0.9; 0.6	001; 002; 003

[a] From the undoped matrix.

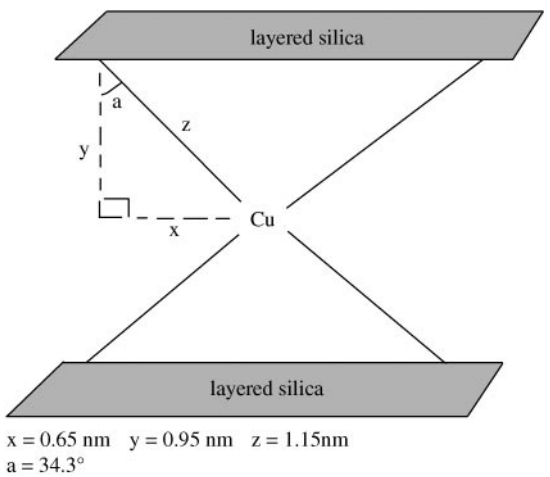

FIG. 3. Schematic representation of the coordination geometry of *n*-alkyldiamine chains in the 10.0-mmol-doped hybrid.

coordination number of copper are associated with the different colors exhibited by the samples. For example, the LSCu2 sample, with the largest proportion of copper, certainly exhibits a small amount of amine molecules coordinated to each metal cation, whereas the reverse behavior can be inferred for the LSCu1 matrix with lower copper content.

The addition of manganese chloride drastically reduces the original structure of the matrix and only a diffraction peak at 5.8°, which is attributed to the 001 plane, can be observed. The same phenomenon is observed for cobalt-modified matrix with the correspondent 001 diffraction peak at 5.9°.

The synthesized hybrid containing nickel showed both 001 and 002 diffraction peaks at 5.6° and 11.4°, respectively. This result is in agreement with the lamellar nature of the matrix being maintained in this case. However, a weak diffraction peak at 3.8° can be observed due to the 001 diffraction plane of the original hybrid. This fact is an indication that not all silica sample were doped with this cation.

The effects caused by addition of cadmium and mercury chlorides to the original matrix are very similar, as can be seen by inspection of Figs. 4 and 5. The matrix involving cadmium showed diffraction peaks at 4.9°, 9.7°, and 14.6°, whereas the matrix containing mercury exhibited the same sequence of peaks at 4.8°, 9.6°, and 14.4° (Table 2). The observed diffraction peaks are due to the 001, 002, and 003 diffraction planes, in both cases. On the other hand, the zinc-modified matrix showed only two diffraction peaks at 5.8° and 6.7°. The first can be attributed to the 001 diffraction plane, but the second cannot be confidently assigned. So, addition of cadmium and mercury disturbs the original structure of the matrices to a low extent, compared with addition of zinc. The presence of cadmium and mercury caused the 002 and 003 diffraction peaks, especially the latter, to have very well defined profiles compared with the original hybrid.

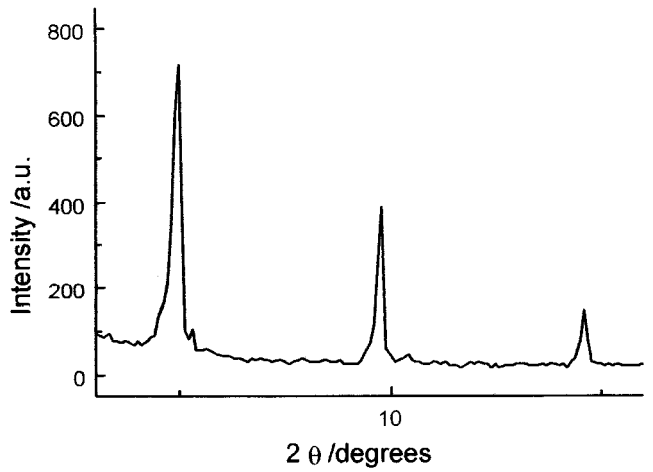

FIG. 4. X-Ray diffraction pattern of lamellar silica doped with 10.0 mmol of $CdCl_2$.

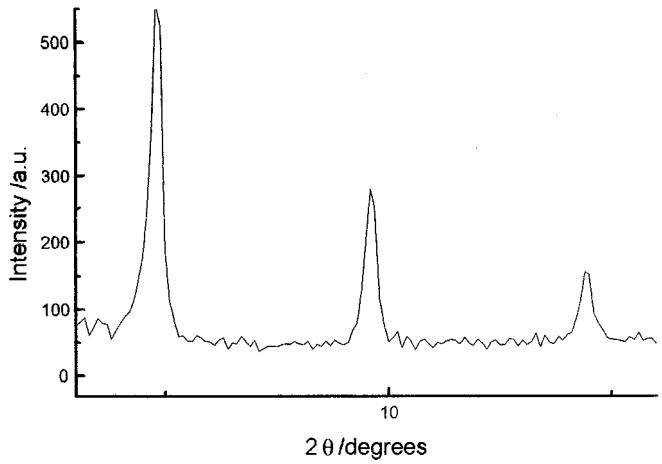

FIG. 5. X-Ray diffraction pattern of lamellar silica doped with 10.0 mmol of $HgCl_2$.

The similarity in behavior exhibited by cadmium and mercury contrasts with that of zinc. This feature can be understood in terms of the coordination properties associated with these three elements. The intermediate position of cadmium in the group leads to a similarity in properties to mercury, the stereochemical coordination behavior of which is distinct from that of zinc (23). In this direction, the same sort of arguments can be used to rationalize the similarity of other cations, as was observed for the first row of transition elements, represented by manganese and cobalt. However, a discrepancy is related to the addition of iron(III) chloride to the original hybrid, which resulted in a completely amorphous material.

Thermogravimetry is a reliable analytical tool for characterizing quantitatively silica gel (24) or organically modified (25) silica samples. Then, from the mass losses on the curves obtained, the silica/organic moiety ratios of the synthesized hybrids were calculated. These thermogravimetric results are summarized in Table 3. The total mass released corresponded not only to the carbonic chain but also to the cations complexed. Thus, the silica/organic moiety ratio decreased as the molar mass of the cation or the total amount of coordinated cation increased. One expressive illustration of this behavior occurred with cobalt and nickel hybrids, which gave close ratios due to the proximity of the cation molar mass values.

The thermogravimetric curves for the original lamellar silica and nickel-doped matrices are shown as illustrative examples in Figs. 6 and 7, respectively. Some hybrids presented a first step of mass loss due to the release of physisor-

TABLE 3

Mass Percentage of Silica Substrate, SiO_2, Silica Substrate/Organic Moiety Ratio, (SiO_2/organic) for the Original Lamellar Silica (SL) and the Hybrids Containing *x* mmol of cation *M* (*xM*), Obtained by Thermogravimetry

Matrix	SiO_2 (%)	SiO_2/organic
SL	53	1.13
10.0Mn	48	0.92
10.0Co	33	0.49
10.0Ni	33	0.49
10.0Cu	37	0.59
15.0Cu	32	0.47
10.0Zn	29	0.41
10.0Cd	25	0.33
10.0Hg	13	0.15

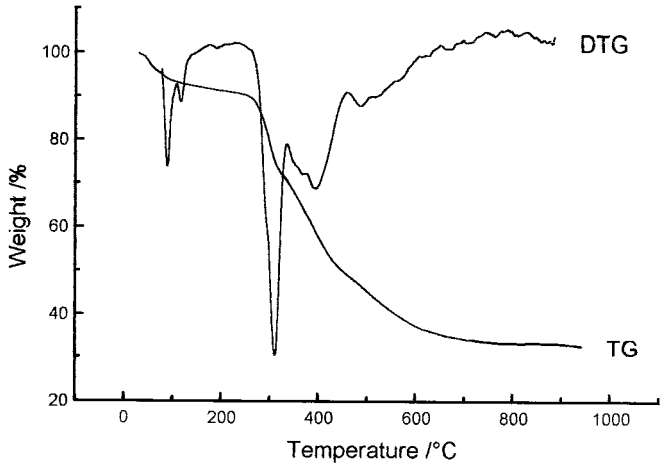

FIG. 7. Thermogravimetric curve and the corresponding derivative curve of 10.0 mmol of $NiCl_2$ in the lamellar silica hybrid.

bed water molecules, and then, it was not considered as a measure of the thermal stability.

The general behavior is in agreement that the addition of metal chlorides yielded hybrids with enhanced thermal stability, compared with the original matrix. The temperatures of degradation started at 93, 130, 163, 152, 119, 250, 313, 175, and 180°C for lamellar silica, copper hybrids containing 10.0 and 15.0 mmol, and Mn, Co, Ni, Zn, Cd, and Hg hybrids containing 10.0 mmol, respectively.

The consecutive release of diamine molecules leads to transitions in the solid-state phase such as lamellar → hexagonal → amorphous (16, 17, 22). For the original lamellar silica sample, the first and third mass loss steps are associated with structural transitions corresponding to the sequence lamellar → hexagonal and hexagonal → amorphous. These series of events can be followed by X-ray diffraction data of samples calcined at 200 and 500°C. The hexagonal → amorphous transition is associated with an enthalpic value of 1.8 kJ g^{-1}, a value determined with the DSC curve presented in Fig. 8. In Figs. 9 and 10 are shown the X-ray diffraction patterns of LS calcined at 80 and 200°C respectively, for 3 h. The sample calcined at 80°C retained its lamellar structure, as can be observed by the presence of the 001 and 002 difraction peaks. On the other hand, the sample calcined at 200°C underwent a lamellar-to-hexagonal structural transition, since only the 001 diffraction peak is observed in its X-ray pattern.

The thermogravimetric curves and the respective derivative forms indicated that not only thermal stability changed,

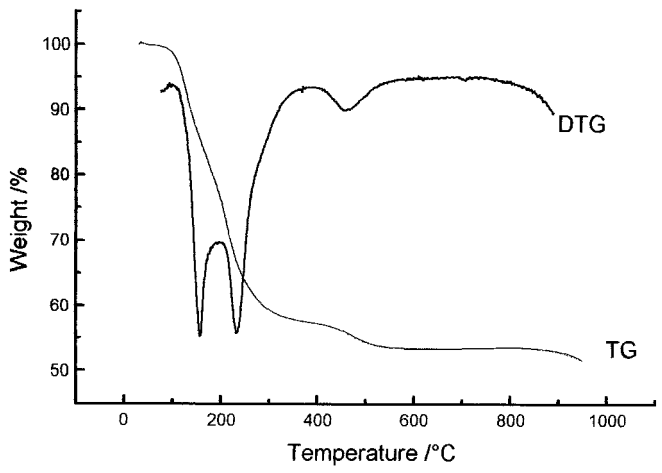

FIG. 6. Thermogravimetric curve and the correspondent derivative curve of the organic–inorganic hybrid of lamellar silica obtained through the neutral amine route.

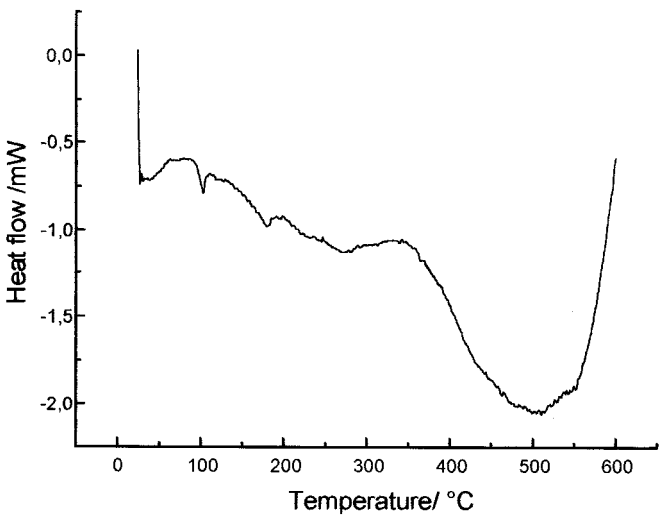

FIG. 8. DSC curve for lamellar silica obtained by the neutral amine route through the sol–gel process.

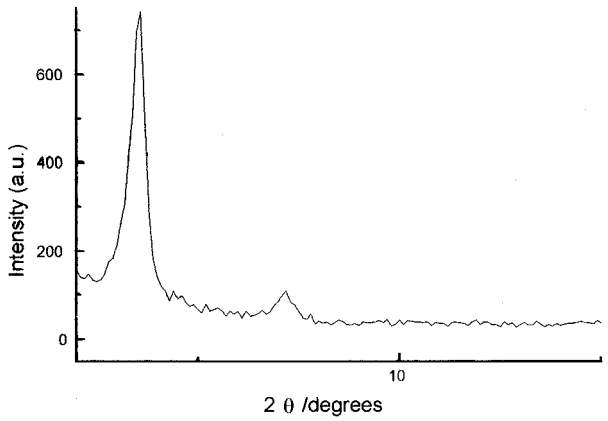

FIG. 9. X-Ray diffraction pattern of lamellar silica calcined at 80°C for 3 h.

but the kinetics of *n*-alkyldiamine chain loss, which is sensible to considerable modifications, also changed. This phenomenon can be explained by remembering that, in metal-doped samples, the *n*-dialkyldiamine chains are lying in the lamellar galleries in coordinating aggregates of variable structure and volume, which means different steric hindrances for distinct samples as well as for different thermal degradation stages. Furthermore, by inspection of TG and DSC curves of the original and hybrid cations samples, the increase in thermal stability of the lamellar phase is followed by a concomitant decrease in the thermal stability of the hexagonal phase. In this connection, the results obtained with copper hybrids, which incorporated the largest amount of doped metal, gave the highest thermal stability for this matrix.

CONCLUSION

The experimental results obtained showed that in general, addition of metal salts increased the thermal stability of the lamellar phase of silica samples, whereas a decrease in the thermal stability of the hexagonal phase was detected. On the other hand, addition of metal salts can have a marked effect on the structure of the obtained materials. This phenomenon can be controlled by the amount used, as well as the coordination features of the specific metal employed, to obtain silica samples with the desired structure and also with a specific thermal stability.

The lamellar silica synthesized here exhibited a significant capacity to bond metal cations selectively, which was proved by comparing, for example, calorimetric results collected for those matrices contained copper and nickel (26). This new proposed route opens an exciting possibility of using this kind of material as a catalyst support and/or selective analytical agent. Furthermore, as recently demonstrated (27) the solid state reaction of copper nitrate- or copper sulfide-doped silica samples with potassium bromide can be used to promote marked structural modifications of silica matrices.

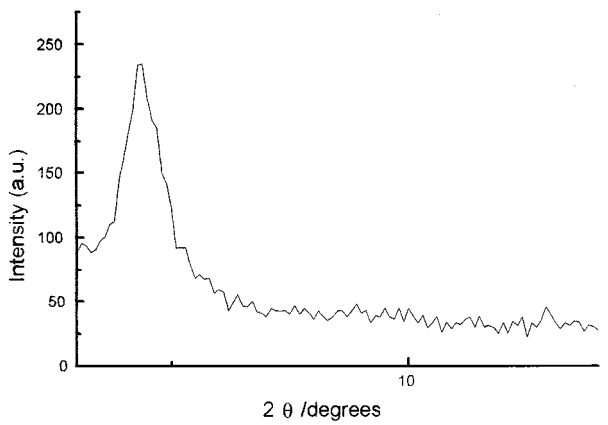

FIG. 10. X-Ray diffraction pattern of lamellar silica calcined at 200°C for 3 h.

ACKNOWLEDGMENTS

The authors are indebted to FAPESP for financial support and CAPES-PICDT and CNPq for a fellowship.

REFERENCES

1. C. J. Brinker and G. W. Scherer, "Sol–Gel Science." Academic Press, New York, 1990.
2. J. Oh, H. Imai, and H. Hiroshi, *Chem. Mater.* **10,** 1582 (1998).
3. P.-H. Sung and T.-F. Hsu, *Chem. Mater.* **10,** 1642 (1998).
4. H. Yang, N. Coombs, and G. A. Ozin, *Nature* **386,** 692 (1997).
5. P. T. Tanev and T. J. Pinnavaia, *Science* **276,** 865 (1995).
6. H. Yang, N. Coombs, I. Sokolov, and G. A. Ozin, *Nature* **381,** 589 (1996).
7. H. Yang, A. Kuperman, N. Coombs, S. Afara-Mamiche, and G. A. Ozin, *Nature* **379,** 703 (1996).
8. Y. Lu, R. Gangull, C. A. Drewien, M. T. Anderson, C. J. Brinker, W. Gong, Y. Guo, H. Soyez, B. Dunn, M. H. Huang, and J. I. Zink, *Nature* **363,** 364 (1997).
9. M. Trau, N. Yao, E. Kim, Y. Xia, G. N. Whitesides, and I. A. Aksay, *Nature* **390,** 674 (1997).
10. J. S. Beck, J. C. Vartuli, W. J. Roth, M. E. Leonowicz, C. T. Kresge, K. D. Schmitt, C. T.-W. Chu, D. H. Olson, E. W. Sheppard, S. B. McCullen, J. B. Higgins, and J. L. Schlenker, *J. Am. Chem. Soc.* **114,** 10834 (1992).
11. C. T. Kresge, M. E. Leonowicz, W. J. Roth, J. C. Vartulli, and J. S. Beck, *Nature* **359,** 710 (1992).
12. M. Ogawa, *Langmuir* **13,** 1853 (1997).
13. M. Ogawa, T. Igarashi, and K. Kuroda, *Bull. Chem. Soc. Jpn.* **70,** 2833 (1997).
14. A. Shimojina, Y. Sugahara, and K. Kuroda, *Bull. Chem. Soc. Jpn.* **70,** 2847 (1997).
15. M. Ogawa, *Chem. Commun.*, 1145 (1996).
16. N. Ulagappan, N. Battaram, C. N. Raju, and C. N. R. Rao, *Chem. Commun.*, 2243 (1996).
17. P. T. Tanev and T. J. Pinnavaia, *Science* **271,** 1267 (1996).
18. H. A. Flaschka, "EDTA Titrations." Pergamon Press, New York, 1964.

19. G. E. Maciel and D. W. Sindorf, *J. Am. Chem. Soc.* **102,** 7606 (1980).
20. D. W. Sindorf and G. E. Maciel, *J. Am. Chem. Soc.* **105,** 1487 (1983).
21. R. M. Silverstein, G. Clayton Bassler, and T. C. Morril, "Spectrometric Identification of Organic Compounds." Wiley, New York, 1991.
22. Neeraj and C. N. R. Rao, *J. Mater. Chem.* **8,** 1631 (1998).
23. N. N. Greenwood and A. Earnshaw, "Chemistry of the Elements." Butterworth–Heinemann, Cambridge, 1984.
24. R. F. de Farias and C. Airoldi, *J. Therm. Anal.* **53,** 751 (1998).
25. A. R. Cestari and C. Airoldi, *J. Therm. Anal.* **44,** 79 (1995).
26. R. F. de Farias and C. Airoldi, unpublished results.
27. R. F. de Farias and C. Airoldi, *J. Non-Cryst. Solids*, in press.